Crystallization

DOI: 10.1002/ange.201102814

On the Nature of Chirality Imparted to Achiral Polymers by the Crystallization Process**

*Martin Rosenthal, Georg Bar, Manfred Burghammer, and Dimitri A. Ivanov**

The control of spatiotemporal patterns in self-organized chemical systems, such as the classical Belousov–Zhabotinsky reaction, has been the focus of many experimental and theoretical works.[1] In polymer science, periodic dissipative patterns resulting for example from non-equilibrium processing conditions, such as solvent evaporation and crystallization, are sometimes observed.[2] However, most remarkably, semicrystalline polymers have a unique intrinsic capability of forming long-range-order morphological patterns, that is, banded spherulites. These morphological features can be repeatedly formed upon crystallization from the melt and are therefore largely independent from the initial film processing conditions, such as the solvent used for casting or film thickness.[3] The banded spherulites may be as large as several centimeters in diameter, whereas the width the band is on the order of micrometers (Figure 1 A). By now, it is widely accepted that the banded spherulite morphology stems from formation of nonplanar polymer crystals and, in particular, from twisting of the crystalline lamellae during their growth to form left- and right-handed helicoids or helices. Therefore in the case of achiral polymers, the chiral character of the resulting supramolecular objects, such as the helicoidally-shaped crystalline lamellae, is imparted to them by the crystallization process. Even if the interpretation of the banded spherulite morphology (Figure 1 A) as a result of lamellar twist is well-accepted by now,[4] the origin of lamellar curving during crystal growth is not yet fully clear. Despite extensive studies conducted in this field for more than half a century, it is still a topic of ongoing interest and controversy.[5]

The main objective of the present study is to identify the chiral parameter added to the system by the crystallization process using the example of high-density polyethylene (HDPE), which is the archetypal flexible-chain polymer. In the crystalline state, HDPE adopts a planar zigzag conformation with regular mirror planes running perpendicular to the chain direction, that is, the chain conformation is achiral. This means that chirality of the crystalline lamellae cannot be induced by the chain conformation in the crystalline lattice. The idea that surface stresses can lead to lamellar twisting goes back to the early 1960s when Geil[3] analyzed the impact of the crystal surface on the lamellar geometry and pointed to the fact that thin lamellar crystals can bend when surface strains are present. A qualitative model suggesting the existence of unbalanced surface stresses was later introduced by Keith and Padden[6] (KP model), who developed it specifically for the case of HDPE. Moreover, the authors suggested that the basic principles of the model can be transferred to other semicrystalline polymer systems, and are thus of general character. Figure 1 B shows the distribution of surface stresses on the crystalline lamella surface, according to the KP model. When viewed from the growing lamellar tip the sectional shape of the lamellar crystal corresponds to a parallelepiped. Here the crystalline stems make an obtuse angle on one fold surface while it is acute on the other. According to the intuition of Keith and Padden this results in different chain-fold conformations. The chain fold is assumed to be more sterically hindrant when the chain overhangs the growth front, or has to fold about an acute angle, leading to a

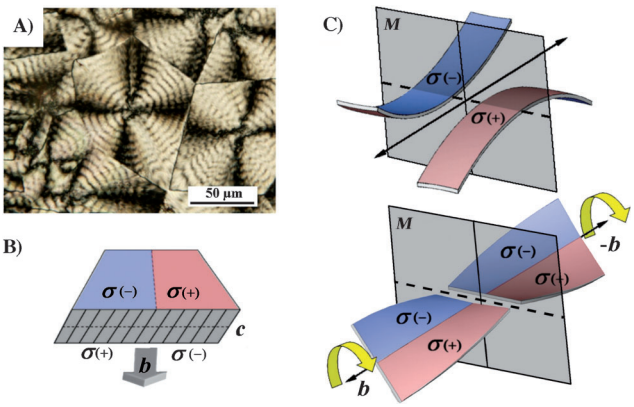

Figure 1. A) Polarized optical micrograph of banded polyethylene spherulites melt-crystallized at 105 °C. B) Representation of a crystalline lamella with the stems inclined by a significant angle with respect to the lamella normal, which gives rise to generation of the surface stress σ, according to the Keith and Padden model.[6a,b] C) Sketch showing bending of the two lamellar halves with opposite surface stress asymmetry (top). The unbalanced surface stresses result in a helicoidal lamellar shape symmetric about the mirror plane *M* perpendicular to the crystal growth direction and passing through the primary nucleus (bottom).

[*] Dr. M. Rosenthal, Dr. D. A. Ivanov
Institut de Sciences des Matériaux de Mulhouse, CNRS
15 rue Jean Starcky, 68057 Mulhouse (France)
E-mail: dimitri.ivanov@uha.fr
Dr. G. Bar
Analytical Technology Center, Analytical Technologies
Dow Olefinverbund GmbH
06258 Schkopau (Germany)
Dr. M. Burghammer
European Synchrotron Radiation Facility
6 rue Jules Horowitz, 38043 Grenoble (France)

[**] We are grateful to Bernard Lotz for donation of the Sclair sample and for very fruitful discussions. We acknowledge the financial support of the French Agence Nationale de la Recherche Scientifique (ANR) in the frame of project "T2T".

Supporting information for this article is available on the WWW under http://dx.doi.org/10.1002/anie.201102814.

positive surface pressure $\sigma(+)$. By contrast, the fold is supposed to consume less space when it loops around an obtuse angle, giving rise to a negative value of $\sigma(-)$. It has to be mentioned that the indicated surface stresses $\sigma(+)$ and $\sigma(-)$ should not be considered as the absolute values; rather, they only indicate a relative difference responsible for the buildup of the unbalanced stresses. The qualitative arguments of Keith and Padden[6] and their explanations supporting this view are however far from being rigorous, and were criticized in the literature.[5]

Alternate explanations than those suggested by Keith and Padden are also described. For example, Bassett[7] emphasizes the dynamics and sequence of molecular processes taking place in polymer lamellae suggesting that at the growth front the chain tilt is not present in the lamellar crystals and therefore cannot be the main origin of twisting. However, the exact difference in the fold conformation on the opposite fold surfaces and the chronology of the molecular processes can be of secondary importance for the present study, which analyzes only the resulting structure.

Figure 1C depicts the mirror plane symmetry of the lamellar crystal, which spreads from the primary nucleation center simultaneously in the b and $-b$ directions. If the two halves of the lamella were split along the long lamellar axis (Figure 1C, left), they would bend according to the sign of the surface stress, as proposed by Keith and Padden. Since in reality both halves stay connected, the opposite bending moments exerted on them impose a torque, which results in twisting of the entire lamella around the growth axis. Importantly, the sense of the torque and thus the handedness of the twist are different for the positive or negative growth-axis polarity. Thus for the case illustrated in Figure 1B,C, the lamellar helicoid is left-handed when it grows in the positive b direction while it has to be right-handed when growing in the negative, or $-b$, direction. This can be readily figured out from the mirror-plane symmetry operation, which inverts the handedness of the helicoid. Therefore the sense of the lamellar twist is directly correlated to the direction of the chain tilt thereby suggesting that the latter is likely to be the searched for "chirality" parameter imparted to the lamellar structure of achiral polymers, such as HDPE by crystallization. To check this premise of the KP model, we employed microbeam X-ray scattering with an X-ray beam size significantly smaller than the spherulite bandwidth.

It is noteworthy that this technique has previously been used to identify the crystal growth axis and local crystal orientation in banded and non-banded spherulites of poly(L-lactic acid),[8a] poly(3-hydroxybutyrate),[8b] it-polystyrene,[8c] it-poly(butene-1),[8c] and poly(trimethylene terephtahlate).[8d] The theoretical approaches for the analysis of the helicoidal lamellar shapes based on microfocus X-ray patterns were introduced recently.[9]

Typical 2D microfocus X-ray patterns averaged over one radial scan through the whole HDPE spherulite are shown in Figure 2. These patterns correspond to the two different sample-to-detector distances that were used to visualize WAXS and combined SAXS/WAXS angular regions. The appearance of the patterns suggests uniaxial sample symmetry, as it is often found for example for drawn fibers. However,

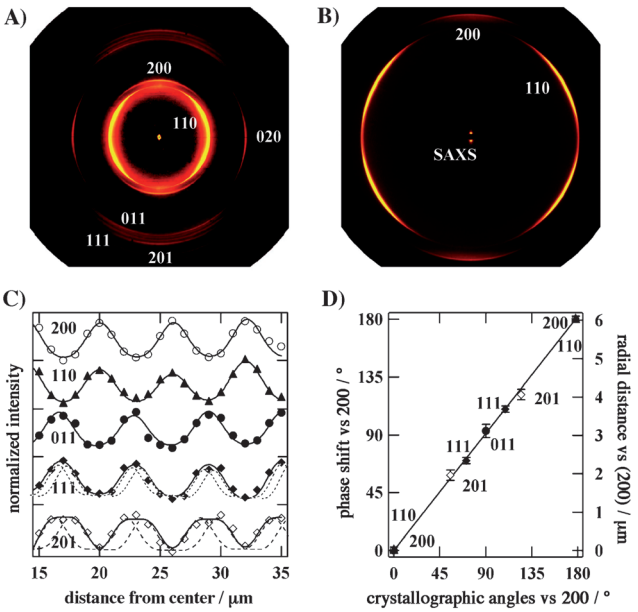

Figure 2. A) Averaged 2D X-ray pattern recorded during a horizontal radial scan across the whole HDPE spherulite. The 020 reflection stays equatorial showing the constancy of the crystal growth direction. The 200 reflection rotates in the plane perpendicular to the growth axis. B) Averaged 2D X-ray pattern measured at a larger sample-to-detector distance exhibits two-spot SAXS signal, reflecting regular stacking of the radial lamellar crystals. C) Intensity of the strongest reflections versus radial distance from the spherulite center. The values correspond to the average of the intensity recorded on the bottom and top detector halves. D) Radial distance and phase shift of the reflections shown in (C) versus the crystallographic angle of the corresponding reciprocal space vectors with respect to the 200 vector in the (010) plane.

in the case of the microfocus patterns, the preferred axis does not correspond to the chain axis of the polymer but to the crystallographic fast-growth axis. The $h0L$ reflections are located on the meridional direction of the pattern, while the 020 reflection is positioned on the equator, which means that the crystal growth axis (that is, the equator of the diffractogram) is parallel to the b direction of the HDPE orthorhombic unit cell. This is in agreement with the literature data.[3] Importantly, the diffraction patterns recorded at a larger sample-to-detector distance (Figure 2B) allow observing the SAXS signal resulting from the lamellar stacks in the edge-on orientation. The corresponding long period of the semicrystalline structure of HDPE equals approximately 15 nm. The SAXS signal provides additional information as to the orientation of the polyethylene chains with respect to the normal to the lamellar basal plane.

The normalized intensity of the most intense reflections located on the meridian and on the first and second layer lines of the patterns are given in Figure 2C. It can be seen that, when plotted as a function of the radial distance, the intensities exhibit a regular oscillation behavior for the peaks periodically enter and exit the reflection conditions. The latter are reached at different radial positions for the different peaks, as it is expected for a single crystal simultaneously rotated and translated about one of the axes. The

oscillation period equals (6.0 ± 0.1) μm, which is in agreement with the value derived from the optical micrograph in Figure 1 A.

The 200 reflection shows up once per half turn of the lamella, as it is expected. The meridional *h0L* reflections appear twice per half turn, forming two doublets in the meridional plane. By contrast, the mixed *hk*0 and 0*kl* reflections appear only once per half turn. Although these peaks present a four-spot pattern (quadruplet) on the diffractogram, they do not have a phase lag between their counterparts if the effect of the finite curvature of the Ewald sphere is neglected, which will be discussed later. Finally, the *hkl* reflections such as 111 appear twice per half turn because it can be viewed as a pair of quadruplets such as {*hkl*, *h*−*kl*, −*hk*−*l*, −*h*−*k*−*l*} and {*hk*−*l*, *h*−*k*−*l*, −*hkl*, −*h*−*kl*}, each of which show up simultaneously on the diffractogram.

In full analogy with a single HDPE crystal twisting during growth about its *b* axis, the phase shifts of the different reflections can be calculated from the radial distances at which they reach their maximum intensity normalized by the helicoid period (or twice the band spacing visible in the optical micrograph). These phase shifts can be then compared to the angles between the projections of the corresponding reciprocal space vectors onto the plane perpendicular to the *b* direction with respect to any reference vector in this plane such as 200 (Figure 2 D). It can be seen that the obtained dependence exactly follows the line $y = x$, which means that the crystal rotation is continuous and regular. This conclusion is not that obvious as it may seem because in the past it was suggested that the lamellar twist in PE occurs in a stepwise manner. Thus Bassett and Hodge[10a,b] concluded from microscopy data that the polyethylene lamellae stayed untwisted over about one third of the band spacing and afterwards exhibited an abrupt variation of the *c* axis orientation owing to a sequence of screw dislocations of consistent sign. It is clear that our X-ray data does not provide support to these findings.

A more detailed analysis of the lamellar microstructure can be carried out based on the results of combined SAXS/WAXS experiments. Figure 3 A shows the intensity and azimuthal position of the meridional 200 and SAXS peaks. Note that the same data in the averaged form is already given in Figure 2 C. The 200 peak showing up at the azimuth of 90° corresponds to the reflection appearing in the top part of the detector while the one at 270° corresponds to the one in the bottom part. Thus, it is apparent that, over the whole radial scan, the two reflections stay strictly meridional (that is, at 90 and 270°). This signifies that the lamella shape corresponds to a helicoid rather than to a helix because in the latter case wagging of reflections about the meridional direction is expected. Since the Ewald sphere has a notable curvature for the wavelength used, the centrosymmetric counterparts of the meridional reflections (for example, 200 and −200) should appear at slightly different moments while the crystal rotates around the growth axis. The angle between them corresponds to twice the Bragg angle 2θ (see the Supporting Information). The separately integrated intensities of the 200 and −200 counterparts are given in Figure 3 B (bottom) as a function of distance from the spherulite center. Both reflections show

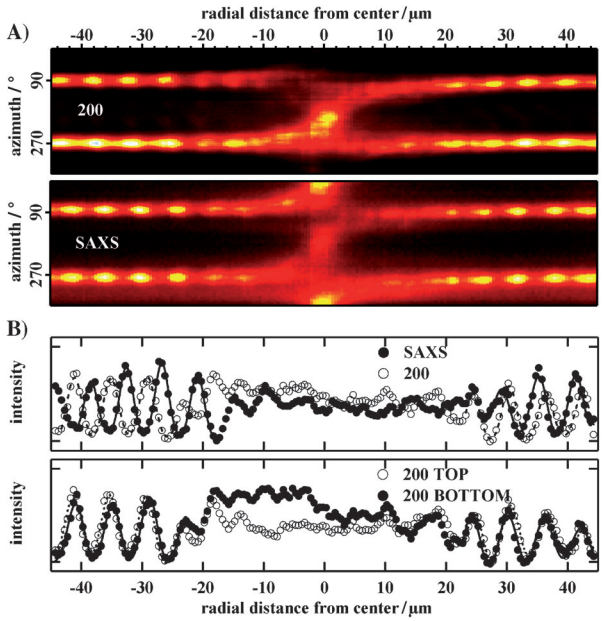

Figure 3. A) Azimuthal position of the meridional 200 reflection (top) and SAXS signal (bottom) versus radial distance from the spherulite center. B) 1D plots of the scattering intensities shown in (A) reveal that when looked from the spherulite center outwards, the SAXS signal reaches its maximum at approximately one-third of the band spacing before the 200 reflection (top). Comparison of the two centrosymmetric counterparts of the 200 peak appearing at the bottom and top halves of the detector.

periodic oscillations except in the region of the spherulite center where, owing to a finite film thickness, the helicoids can grow at oblique angles with respect to the film surface resulting in misorientation of the reflections.

Inspection of the peak positions reveals that the reflection visible on the bottom segment of the detector appears slightly before its counterpart on the detector top segment. Analyzing this fact with the help of the Ewald sphere construction (see Supporting Information), we can deduce that the crystal twist sense is right-handed for its section grown to the left of the spherulite center while it is left-handed on the right half of the spherulite. Repeating this analysis on microfocus scans performed across ten different HDPE spherulites showed that none of the two handednesses is preferred and that both left- and right-handed lamellar helicoids can be observed within the same polyethylene spherulite.

The exact orientation of the HDPE unit cell within the lamella can be found from the phase shift of the SAXS signal with respect to the WAXS peaks of the crystalline lattice. The normalized intensity of the 200 and SAXS peaks are given as a function of the spherulite radius in Figure 3 A. Apart from the central region of the spherulite, the SAXS signal appears before the 200 reflection when looking from the spherulite center outwards. The lateral shift is (1.16 ± 0.07) μm, which corresponds to a chain tilt of $(34.6 \pm 2.0)°$ (Figure 4 A). Thus the fold surface of PE in the bulk can be assigned to the (201) plane.

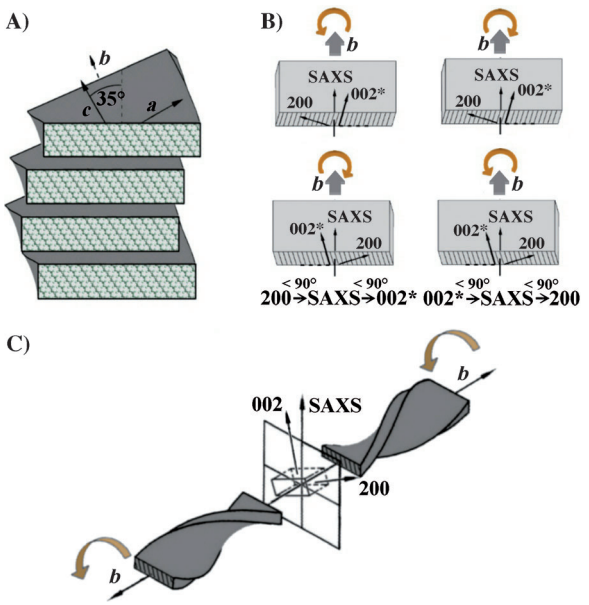

Figure 4. A) Orientation of the HDPE unit cell relative to the lamellar basal plane. The crystalline stems are tilted by about 35° with respect to the lamellar normal along the *a* direction. For a given element of the lamellar stack, the chain tilt has a unique direction in space. B) Totally four different combinations of the chain tilt and lamellar twisting sense can be imagined. The asterisk beside 002 indicates that this reflection was not observed in the experiment. C) Vector model illustrating the rotating unit cell of HDPE. The axis of rotation corresponds to the crystallographic *b* axis. The *k0L* reflections rotate in the (010) plane. The curved arrows indicate the rotation direction of the unit cell.

As mentioned above, the considered crystallographic reflections as well as the SAXS signal appear only once per half turn of the lamellar stack, indicating that the chain direction is unique across the whole lamellar stack. This result is at variance with what is known for example for HDPE single-crystal mats, where both chain tilts (that is, to the left and right from the lamella normal) are statistically present. The presence of two directions of the crystalline stems brings about angular splitting of the 200 reflection with respect to the plane of the sample when the X-ray beam is shined parallel to the lamellar surface.[3] Thus, contrary to single-crystal mats,[11] the twisting lamellar stacks of bulk HDPE reveal a single-crystal-like texture (Figure 4A).

To verify the premise of the KP model about the added chirality parameter, the direction of the chain tilt has to be correlated to the rotation direction of the crystal (Figure 1B,C). In total, there are four possible situations (Figure 4B). In the upper row of Figure 4B, the chains in the lamellae are tilted to the right from the lamella normal, while in the bottom row they are tilted to the left. The structures depicted in the left and right columns will generate the diffraction peaks with a different order of appearance when performing the microfocus X-ray scans in the radial direction from the spherulite center outwards. As mentioned above, the KP model predicts the formation of structures corresponding to the following order of the peak appearance: 002→SAXS→200, that is, the ones in the right column in Figure 4B. Even if in the experiment the 002 reflection was not observed owing to insufficient angular range, it is rather straightforward to derive the chain direction by taking into account the fact that if the angle between 200 and SAXS signals is less than 90°, the chain direction will either precede or follow the SAXS peak (depending on which of the two peaks shows up first), being separated from it by the complementary angle (Figure 4B). For all microfocus scans performed in this work, we always recorded only one order of the peak appearance, which is 002→SAXS→200. This unambiguously shows that the hypothesis of Keith and Padden is correct. Therefore, in principle information on the lamellar handedness would not even be needed to verify the premise of the KP model.

However, the fact that left- and right-handed helicoids are present shows that crystals can grow in both *b* and $-b$ directions (Figure 4C), which are however indistinguishable crystallographically owing to the high symmetry of the HDPE unit cell. We indeed often observe that crystals growing to the opposite sides of the spherulite center have opposite handedness. The division of type 2 spherulites into two homochiral fields symmetric about a vertical plane passing through the spherulite center has been previously reported using AFM imaging[12a] and a combination of AFM and a circular-extinction microscope.[12b] However, in our case the handedness inversion is not observed for all the scans because the scan may cross not only the well-organized sheaf-like part of the initial immature spherulite but also the less-ordered spherulitic "eyes" formed during later in-filling lamellar growth.[4]

It is important that, once defined, the handedness of the lamellar helicoid does not change anymore during its radial growth, as it is coupled to the direction of the chain tilt.

Summarizing, the crystallization process imparts to achiral polymers an additional chiral parameter, which allows them to form chiral supramolecular structures such as left- and right-handed lamellar helicoids. Using microfocus X-ray diffraction with the X-ray beam footprint smaller that the characteristic lamellar twisting period, we have shown with the example of HDPE that the added chiral parameter is the chain tilt direction with respect to the lamellar normal. Thus, when looking along the crystal growth direction the lamella having the crystalline stems tilted to the right from the normal to the lamellar basal plane will form a right-handed helicoid, whereas the lamella with the stems tilted to the left will be left-handed. This finding is in agreement with the model of Keith and Padden. An interesting consequence of such crystallization-imparted chirality is that it can be considered as a bit of morphological memory (left)/(right) that chiral polymer lamellae transfer during their radial growth over several hundred micrometers and more.

Experimental Section

The present study was conducted on free-standing films of unfractionated linear PE (DuPont Sclair 2901, $M_w = 72000\ g\,mol^{-1}$, $M_n = 19500\ g\,mol^{-1}$) melt-crystallized at 105 °C. The choice of the sample is based on its reputed low nucleation density[5] allowing to grow relatively large banded spherulites. The film was processed between cover glass slips to ensure a uniform film thickness of about 20 μm.

After immersion in 1% HF aqueous solution for 2 h, the films where floated off on water. Microbeam X-ray scattering experiments were carried out at the ID13 beamline of the European Synchrotron Radiation Facility (ESRF) in Grenoble, France. The measurements were performed in transmission, with the sample surface normal to the X-ray beam, using the crossed-Fresnel optics and the wavelength of 1.0 Å. The spot size of the monochromatic X-ray beam at the focus point was about 1.5 μm along the horizontal axis and 2.0 μm along the vertical axis. The norm of the scattering vector s ($s = 2\sin(\theta)/\lambda$) was calibrated using several diffraction orders of corundum. The sample was scanned by means of an x–y gantry. The diffraction patterns were collected using a step of 0.5 μm.

Received: April 22, 2011
Revised: July 13, 2011
Published online: August 25, 2011

Keywords: chirality · crystallization · lamellar twisting · polyethylene · polymers

[1] A. S. Mikhailov, K. Showalter, *Physics Reports* **2006**, *435*, 79–194.
[2] T. Okubo, J. Okamoto, S. Takahashi, A. Tsuchida, *Colloid Polym. Sci.* **2009**, *287*, 1155–1165.
[3] P. H. Geil, *Polymer Single Crystals*, *John Wiley and Sons Inc.*, *New York*, **1963**.
[4] U. W. Gedde, *Polymer Physics*, *Chapman & Hall*, *London*, **1995**.
[5] B. Lotz, S. Z. D. Cheng, *Polymer* **2005**, *46*, 577–610.
[6] a) H. D. Keith, F. J. Padden, *Polymer* **1984**, *25*, 29–41; b) H. D. Keith, F. J. Padden, *Macromolecules* **1996**, *29*, 7776–7786.
[7] D. C. Bassett, *Polymer* **2006**, *47*, 3263–3266.
[8] a) M. Gazzano, M. L. Focarete, C. Riekel, M. Scandola, *Biomacromolecules* **2004**, *5*, 553–558; b) M. Gazzano, M. L. Focarete, C. Riekel, M. Scandola, *Biomacromolecules* **2000**, *1*, 604–608; c) H. Kajioka, S. Yoshimoto, R. C. Gosh, K. Taguchi, S. Tanaka, A. Toda, *Polymer* **2010**, *51*, 1837–1844; d) M. Rosenthal, D.V Anokhin, V. A Luchnikov, R. J. Davies, C. Riekel, M. Burghammer, G. Bar, D.A Ivanov, *IOP Conf. Ser. Mater. Sci. Eng.* **2010**, *14*, 012014.
[9] a) V. A. Luchnikov, D. A. Ivanov, *J. Appl. Crystallogr.* **2009**, *42*, 673–680; b) V. A. Luchnikov, D. A. Ivanov, *J. Appl. Crystallogr.* **2010**, *43*, 578–586.
[10] a) D. C. Bassett, A. M. Hodge, *Proc. R. Soc. London* **1978**, *359*, 121-132; b) D. C. Bassett, A. M. Hodge, *Polymer* **1978**, *19*, 469–472.
[11] a) S. Hocquet, M. Dosière, A. Thierry, B. Lotz, M. H. J. Koch, N. Dubreuil, D. A. Ivanov, *Macromolecules* **2003**, *36*, 8376–8384; b) S. N. Magonov, N. A. Yerina, G. Ungar, D. H. Reneker, D. A. Ivanov, *Macromolecules* **2003**, *36*, 5637–5649.
[12] a) A. Toda, T. Arita, M. Hikosaka, J. K. Hobbs, M. J. Miles, *Journ. Macromol. Sci. Part B* **2003**, *B42*, 753–760; b) E. Gunn, R. Sours, J. B. Benedict, W. Kaminsky, B. Kahr, *J. Am. Chem. Soc.* **2006**, *128*, 14234–14235.